Artificial Neural Network Application for Aerodynamics of an Airfoil Equipped with Plasma Actuators

H. Akbıyık[†] and H. Yavuz

Mechanical Engineering Department, Çukurova University, Adana, 01330, Turkey

†*Corresponding Author Email: hakbiyik@cu.edu.tr*

ABSTRACT

Prediction of the aerodynamic forces acting on a NACA 2415 airfoil equipped with plasma actuators is carried out by using artificial neural network. The data sets for ANN model include the experiments which are plasma actuator positions for effective flow control, different Reynolds numbers and various attack angles. Mean absolute percentage and mean squared errors are calculated to assess the performance of the training and the testing stages of ANN model in prediction of drag and lift coefficients. The maximum error for lift and drag estimation are 12.84% and 23.705%, respectively. Also, as a part of the presented study, the process parameters affecting the performance of the plasma actuators in active flow control around a NACA 2415 airfoil is presented in detail. The well-matched results of the ANN based estimations of the ANN indicates that there is almost no need for dealing with complex experimental studies to determine the aerodynamic performance of the NACA2415 airfoil, hence providing the advantage of saving time and cost. Furthermore, the experimental results along with the ability of ANN to estimate aerodynamic performance parameters provide a good database in the active flow control related research field.

Keywords: Airfoil; Plasma actuator; Flow control; Artificial neural networks.

NOMENCLATURE

AoA	Angle of Attack	MAV	Micro Air Vehicle
α_x	output bias value	MSE	Mean Squared Error
AC	Alternate Current	n	number of measured data
AD	cross sectional area for drag force	n_h	number of input parameters
AL	cross sectional area for lift force	Pi	predetermined value
ANN	Artificial Neural Network	R	regression
b	bias value for input layer	Re	Reynolds number
C	chord length	R_i	real measured value
DC	Direct Current	U_∞	mean flow stream velocity
f	plasma excitation frequency	v_j	weight of output value
f_a	activation function for input layer	V_{pp}	peak to peak applied voltage
F	estimated force value	w_{ij}	weight of input layer
FL	measured lift force value	x_c/C	position of the plasma actuators on the airfoil
FD	measured drag force value		
g	activation function for output layer	x_i	input variable
μ	dynamic viscosity	ρ	density of air
MAPE	Mean Absolute Percentage Error		

1.   INTRODUCTION

With the developments in flow control techniques and related technologies, the aerodynamic performance of new generation aircraft systems has been improving ever since. This leads to increasing number of studies on the topic. Some of these studies tackle the issue of increasing

maneuverability, Wang *et al.* (2013), reducing fuel cost with reduced drag, Gad-El-Hak (2000) searching the means for radar hiding, Dorn (1989), improving the aerodynamic forces, Meng *et al.* (2018), Mazaheri *et al.* (2016), Corke *et al.* (2002) and reducing the noise level during take-off, Huang and Zhang (2010). These improvements are achieved by modifying the flow structure around the model. The flow structure is modified by active and passive flow control techniques. In passive methods, Fernandez-Gamiz (2013), Yen *et al.* (2000), Stiesdal and Enevoldsen (2008), Chow and Van Dam (2011), Winzen *et al.* (2014), Fouatih *et al.* (2016), Durhasan *et al.* (2018), there is a geometrical modification and also there is no need for energy. On the other hand, there is a need for energy for active methods, Smith and Glezer (1997), Cattafesta *et al.* (1999), Gunther *et al.* (2007), Güler *et al.* (2018), Messanelli *et al.* (2019), Zhu *et al.* (2019). However, they have the advantage of fast response time to instant system interventions. In this respect, the active flow control devices have an important role in flow structure modification. Plasma actuators, one of the active flow control methods, generate ionized gas and add momentum to the flow around the model. Typically, the generated ions make circular motion from exposed electrode towards embedded electrode side. Consequently, an induced flow occurs and momentum is added to the flow due to collisions of the charged particles with neutral ones, Roth *et al.* (1998), Roth *et al.* (2000), Moreau *et al.* (2006). In active flow control applications, the velocity of induced flow and the actuator flow control performance are the important parameters for improvement of aerodynamic performance. These parameters are related to plasma settings such as the discharge regime, the distance between the electrodes, the width of the exposed and embedded electrode and the type of dielectric material. Dalvand *et al.* (2018) reported experimental investigation, modeling and prediction of transition from uniform discharge to filamentary discharge in DBD plasma actuators by using Artificial Neural Network (ANN). The ANN technique is used for modeling the complex and non-linear system allowing simulation of the system dynamics and related analysis.

The aerodynamic structure of the aircraft wings and the effects of the flow control application play an important role in wind tunnel studies. In such studies, in order to examine these effects and to reveal the related results, there is a need for a number of experiments such as measurements of pressure, velocity, drag and lift. In such a typical experimental study, the requirement for high number of experiments, the experimental system installation costs encourage researchers to carry out numerical studies. Among these numerical studies, ANN has a promising potential due to its capability for modeling complex nonlinear systems, Narendra (1990), Hunt *et al.* (1992), Calise and Rysdyk (1998). In fluid mechanics, ANNs are used mostly for three application areas such as performing image analysis as PIV, Gim *et al.* (2020), Rabault *et al.* (2017), Cai *et al.* (2019), modeling of complex

systems and conducting reduced order modeling, Beck *et al.* (2019), San and Malik (2018), and for performing flow control applications, Rabault *et al.* (2019), Rabault and Khunle (2019), Tang *et al.* (2020), Belus *et al.* (2019).

The use of ANN in aerodynamics is becoming an important design assisting tool as it provides estimation based aerodynamic performance for extreme cases where experimental studies are difficult to achieve. Rai and Madavan (2001) studied the design of turbomachinery airfoils using a neural network that is trained with pressure distribution data. They reported that the usage of the neural network in designing of the airfoils provides a major advantage to designers whom perform to be obligate to work with limits of the design. Faller *et al.* (1994) used ANN to predict the unsteady surface pressure of NACA0015 airfoil. They compared the predicted results with experimental results. They mentioned that, for the aircraft systems integration with sensors, actuators and controllers become far more effective by using ANN. Estimation of aerodynamic properties of aircraft wings and examination of the flow structures around the wings are becoming a regular research topic including such topics as lift coefficient, Post and Corke (2006), drag coefficient, Winslow *et al.* (2018), pressure coefficient, Hand *et al.* (2017), wake region width, Hezaveh *et al.* (2017), etc. Linse and Stengel (1993) reported that aerodynamic coefficients could be identified with neural networks. In addition, ANN can also be used to predict the contribution of active and passive methods used to improve aerodynamic performances. Rokhsaz and Steck (1993a) trained artificial neural network to predict the force and moment coefficients of 70° sweep delta wing. For training the ANN, the experimental data were used in their study. They reported that ANN successfully learn the aerodynamic behavior of the model. Schreck *et al.* (1995) compared the nonlinear and linear structures of the ANN. In comparison study of these structures, a NACA0015 is used as the airfoil model. The temporal and spatial variations are well predicted with ANN using aerodynamic loads and pressure values measured from aircraft wing surface. Kurtulus (2009) successfully studied the prediction of force coefficient for a flapping motion kinematics of a NACA0012 airfoil model. The numerical analysis results of the study are very well matched with the ANN predicted values. Also, it is reported that estimation performance of the ANN appears to be better at lift coefficient than that of the drag coefficient. The ANN training inputs must cover the estimation range with as many datasets as possible. This in turn allows the ANN to get the best prediction of the unknown part of the experimental model data with a higher precision, Rokhsaz and Steck (1993b).

In the first part of the present study, the proposed work aims to show the importance of the DBD plasma actuators. It is shown that these actuators play an important role in control of flow separation and also in improving the aerodynamic forces as a part of active flow control approach. This technique

provides many advantages including fast response time, lack of geometrical change and being on-demand active/passive, etc. In general, ANN performs well in estimation, classification and selection processes within a given data range after an extensive training phase covering the work range. Mainly, the data sets to train the ANN are based on the experimental data or numerical simulation studies. As second a part of the study, the experimental data is presented. This data includes Re numbers from 40000 to 80000 with an increment of 10000. Also angle of attack (AoA) is varied from 0 degree to 17 degree with an increment of 1 degree. In addition, the position of the plasma actuator on the airfoil defined by x_c/C is varied from 0.1 to 0.5 with an increment of 0.1. In order to ensure reliability of the experimental results and to minimize the related errors, each of the experiments are repeated three times. The experimental results along with the ability of ANN to estimate near perfect values of aerodynamic performance parameters provide a good archive database for the research community.

2. ARTIFICIAL NEURAL NETWORK

Artificial Neural Network, as an artificial intelligence technique, is inspired from biological neural systems, Bishop (1994), Dickenson *et al.* (1999). A typical neural network is composed of layers (input, hidden, output) of neurons. Each neuron has a sum with a threshold that is provided by a non-linear mathematical function. Each neuron in a layer takes information from all previous neurons. Then, it sends the sum of received information with considering threshold to all the next layer of neurons. In a Feed-Forward Neural Network (FFNN), the neurons send information only to the following layers. If the neuron sends information back to preceding layers, then it is called a Recurrent Neural Network. The properties of the input layer are determined by the input parameters. The bias and weights of the input layer is optimized by training the ANN for the provided input data. The properties of the output layer are determined by the output parameters. Between input and output layers, there lies the hidden layer number of which can be from one to any counting number depending on the complexity of the input output relation. This structure of network is called multi-layer neural network, as seen in Fig. 1. The ANNs are reported being capable of approximating functions a with desired degree of accuracy provided that sufficiently high number of hidden layers are defined. Hence, ANNs can generally be defined as a class of universal approximators, Hornik *et al.* (1989). It is worth mentioning that the architecture of the Neural Network is critical in predicting and matching the input-output related provided by the experimental data. Hence, it is vitally important to determine the number of inputs, hidden and output layers as well as the type of activation function. In addition, it is worth selecting the appropriate method of training algorithm as well as training, testing and

validation ratios of the overall dataset. The back-propagation algorithm is well-known in the literature, Skapura (1996). Levenberg-Marquardt algorithm is convergent to use with backpropagation algorithm to train ANN. The Levenberg-Marquardt algorithm is the most widely used algorithm for training of neural networks, Hagan and Menhaj (1994). The ANN trained as a part of the study is used for estimation of the aerodynamic output force from the input parameters. The Neural Network based aerodynamic output force calculation is defined as below;

$$F = f_a\left(a_x + \sum_{i=1}^{12} v_j + \left[\sum_{i=1}^{3} g\left(w_{ij}x_i + b_j\right)\right]\right) \qquad (1)$$

where, estimated force value (F), activation function for input layer (f_a), the weight of input layer (w_{ij}), bias value for input layer (b), input variable (x_i), activation function for output layer (g), the weight of output value (v_j), and the output bias value (a_x).

The $\mathrm{tansig(a)}$ in Eq. (2) represents the activation function in the neurons. The output neuron activation function is defined as $\mathrm{purelin(a)}$ function as given in Eq. (3).

$$\mathrm{tansig(a)} = \frac{2}{1+e^{-2a}} - 1 \qquad (2)$$

$$\mathrm{purelin(a)} = a \qquad (3)$$

The input parameters for the ANN is defined as Reynolds number (Re), angle of attack (α), and position of the plasma actuators on the airfoil (x_c/C). The Reynolds numbers are chosen between 4×10^4 and 8×10^4 with an increment of 1×10^4 The presently defined Re range is outlined by Mueller (1999) where the effects of Reynolds number on airfoil maximum sectional lift to drag ratio were shown for MAVs. The force measurement experiments are performed between attack angle of 0 and 17degrees with an increment of 1 degree. The last input parameter used is plasma actuator position on the airfoil surface. The actuators placed on the airfoil surface at x_c/C $0,1$, $0,2$, $0,3$, $0,4$ and $0,5$.

These plasma actuator positions are determined by initial analysis results that takes into account the effect of plasma actuators for flow separation from leading edge to mid-chord of the NACA 2415 airfoil. This argument is also supported the study of Jolibois *et al.* (2008) who have shown that the placement of the plasma actuators leads to more effective separation control when it is mounted on the upstream separation point.

By using the experimental input dataset, the lift and the drag forces acting on NACA2415 airfoil are predicted by the trained ANN. Some studies in the literature divide the dataset into three group as namely as training, validation, and testing, Sarioglu *et al.* (2016) sub-datasets. Some others divide the

H. Akbıyık and H. Yavuz / *JAFM*, Vol. 14, No. 4, pp. 1165-1181, 2021.

dataset into two groups as the training and the testing sub-datasets, Seyhan *et al*. (2017), Ozsahin and Murat (2018).

In order to assess the performance of the developed ANN model, mean squared error (MSE) and mean absolute percentage error (MAPE) methods are

used. As it seen in Eqs. (4) and (5), MSE and MAPE can be given as;
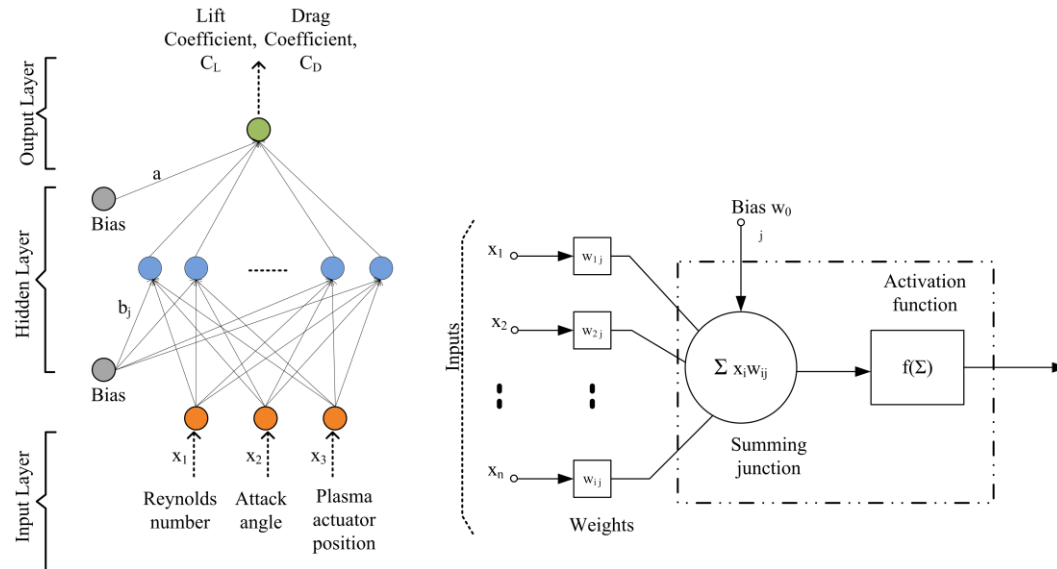
$$MSE = \frac{1}{n}\sum_{i=1}^{n}\left(R_i - P_i\right)^2 \qquad (4)$$

Fig. 1. Schematic description of a multi-layered ANN architecture and scheme of an artificial neuron.

$$MAPE = \frac{1}{n}\sum_{i=1}^{n}\left(\left|\frac{R_i - P_i}{R_i}\right|\right)\times 100 \qquad (5)$$

where, n is the number of measurement data, R_i is real measuring value and P_i is the predetermined value.

3. EXPERIMENTAL RESULTS

Experiments were conducted in an open suction type wind tunnel. The test section of the tunnel is $57cm\times57cm\times100cm$ area as shown in Fig. 2. The main stream velocity was varied from $4.6\,m/s$ and $9\,m/s$. A NACA 2415 airfoil is used as a test model. Its chord and span length are 160 mm and 520mm, respectively.
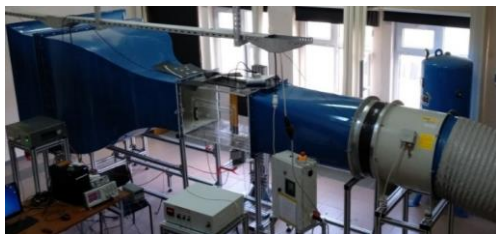

Fig. 2. An open suction type wind tunnel and experimental setup.

The plasma actuator consists of two electrodes and a dielectric material between the electrodes. One electrode that is exposed to the air is applied high

voltage. Other electrode that is encapsulated with the dielectric material is grounded. As it is shown in Fig. 3, the electrodes are copper and their thicknesses are 0.05 mm. The width and length of the electrodes are 5 mm and 520 mm, respectively. The dielectric material is chosen as Kapton that has 3.3 of dielectric constant. The width of the dielectric material is about 10 mm. There is no gap between the embedded and exposed electrodes, where induced flow (plasma) is generated.

The plasma actuators are placed on the surface of the airfoil at $x_c/C = 0.1$, 0.2, 0.3, 0.4, and 0.5 positions. The corners of the electrodes, rounded off around 1mm to prevent burning out of the electrodes, have high electric concentration. The AC frequency supplied to the actuators is applied at 3 kHz and the applied AC voltage is about 8 kV_{pp}. The waveform of the AC signal is selected as a sinus wave. The induced flow is generated by the actuators that are driven by electrical power from custom-made high voltage power supply. A TDS2012B model oscilloscope is used to monitor the signal properties. A Tektronix P6015A model high voltage probe is connected to the oscilloscope in order to acquire for the voltage measurements. Also, the current signal is measured by the oscilloscope using a Fluke 80i-110s AC/DC model current probe.

As it seen in Fig. 3. the airfoil is produced by using 3D printing method with PLA material. A Zortrax M200 model 3D printer machine is used for 3D printing the models. In production process, the diameter of the 3D printer nozzle is selected as a 0.2

mm to achieve a smoother airfoil surface. In order to get 2D flow structure, two end plates are attached to each end of the airfoil model. The diameter of the end plate is chosen as 280 mm. The 60° fillet is applied to the round of end plates.

In this study, the Reynolds numbers are varied from 4×10^4 to 8×10^4 with an increment of 1×10^4. The selection of this range aims at observing flow conditions and variation of aerodynamic forces based on influence of plasma actuators on the air flow. The Reynolds number for the airfoil model used can be defined as;

$$\text{Re} = \frac{\rho \times C \times U_\infty}{\mu} \qquad (6)$$

where, Re is the Reynolds number, C is the total chord length of the NACA 2415 airfoil, μ is the dynamic viscosity, U_∞ is the mean flow stream velocity and ρ is the density of the air.

A six axis ATI Gamma DAQ F/T load cell is used for force measurements. In each force measurement, the results are collected as 2000 samples at a sampling frequency of 100 Hz for the 20 second data recording period. Besides, each experiment is repeated 3 times in order to minimize the experimental error. A rotary unit is used to rotate the airfoil for arrangement of attack angle. The lifting capability of the airfoil is calculated by the lift coefficient given below;

$$C_L = \frac{F_L}{0,5 \times \rho \times U_\infty \times A_L} \qquad (7)$$

where, ρ is the density of the air, U_∞ is the mean flow stream velocity, A is the lifting area of the airfoil, and F_L is the force measured by the load cell. Likewise, the drag coefficient can be defined as;

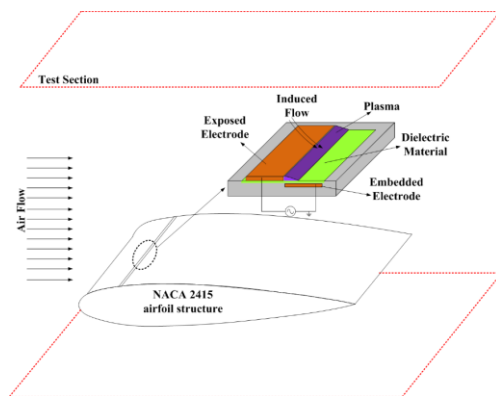$$C_D = \frac{F_D}{0,5 \times \rho \times U_\infty \times A_D} \qquad (8)$$

Fig. 3. A NACA 2415 airfoil structure and produced model.

The MAVs and UAVs have small structure that provides some advantages in application areas such fast maneuvering ability and low radar visibility. The small structure of the MAVs and UAVs leads to smaller control surface. Therefore, they have lower lifting capabilities. The reduced lifting capabilities degrades aerodynamic performance and design of such systems with high aerodynamic performance becomes a challenge. It is worth noting that the plasma actuators play a critical role in improvement of aerodynamic performance of such systems. The plasma actuators are known for their light weight, not requiring geometrical modification and fast response. As reported in the literature, plasma actuators are not only used for increasing the lift coefficient, Akbıyık *et al.* (2017), but also used for decreasing the drag coefficient, Post and Corke (2004) and shifting the stall angle, Moreau (2007). These results are considered as a good contribution to wing's efficiency (CL/CD). It is also reported that plasma actuators are effective in controlling of flow separation, Akbıyık *et al.* (2017), Post and Corke (2004) and reduction in drag at Reynolds numbers between 10×10^3 and 10×10^4. The range of the Reynolds number defined is compatible to the flow conditions of MAVs and UAVs as it is reported by the study of Lissaman (1983), and Mueller (1999).

4. TRAINING OF ARTIFICIAL NEURAL NETWORK

In this study, dataset is divided into two sub-datasets as training (%80 of the dataset) and testing (%20 of the dataset). As a part of the experimental study, a total of 1150 experiments are performed and a total of 350 input data is obtained. This data is then used for training and testing of the ANN model. Figures 4a and 4b show the correlation between the experimental and the predicted values of the drag and the lift coefficient obtained from ANN model.

In the ANN model, the chosen type is defined as three input one output system type. As a part of the ANN training, the number of hidden layers is tested starting from 6 to 15. It has been observed that for the chosen configuration of input and outputs the best fit for lift coefficient estimation is the one with 7 hidden layers while the best fit for drag coefficient estimation is the one with 8 hidden layers.

In a generated ANN model, the determination of hidden layer configuration is a complicated issue and it is highly dependent on the nature of the problem as well as the training data. In literature, one may come across with several solutions for obtaining the number of hidden neuron nodes as well as number of layers based on techniques such as trial-and-error, grid method and some empirical rules, etc. One of approaches for determination of the number of hidden neurons is based on the number of the input parameters (n_h). In literature, these relations are proposed as $2n_h+1$ by Lippmann (1987), and Hecht-Nielsen (1990). While Wong (1991), Tang and Fishwick (1993), and Kang (1991) reports using the relation as 2nh, nh and

(a)
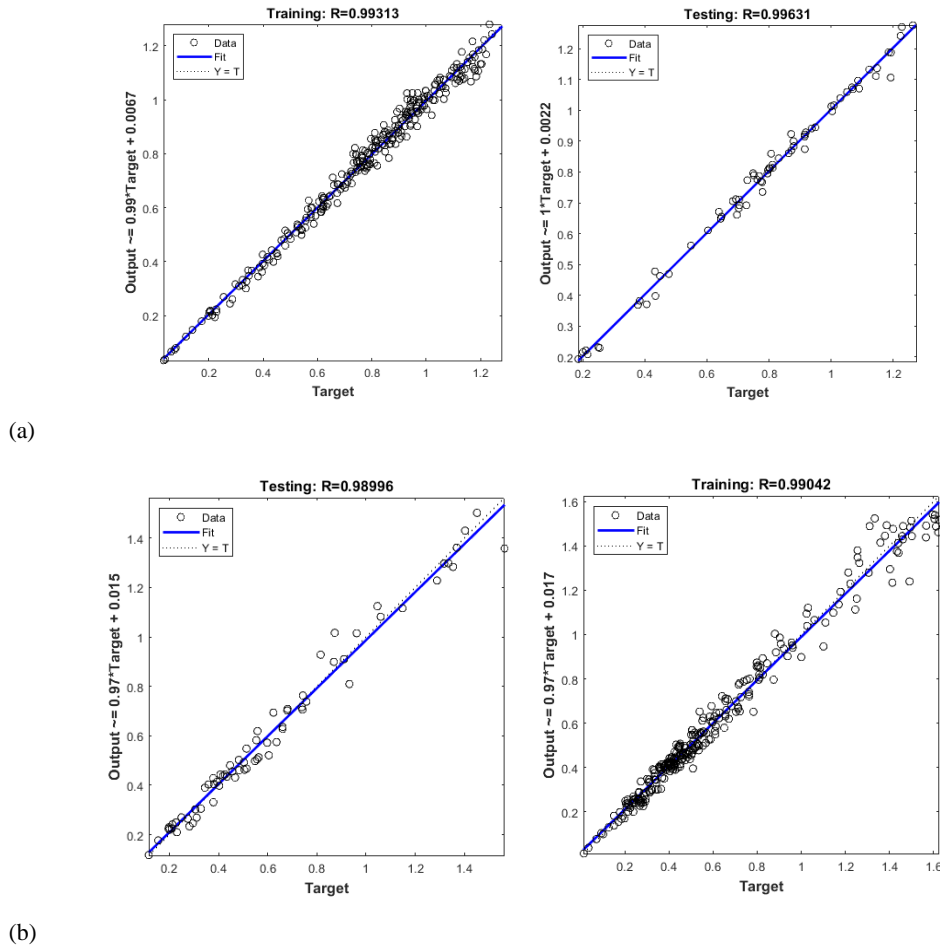

(b)

Fig. 4. Regression models of the training and testing set for a)lift coefficient b)drag coefficient.

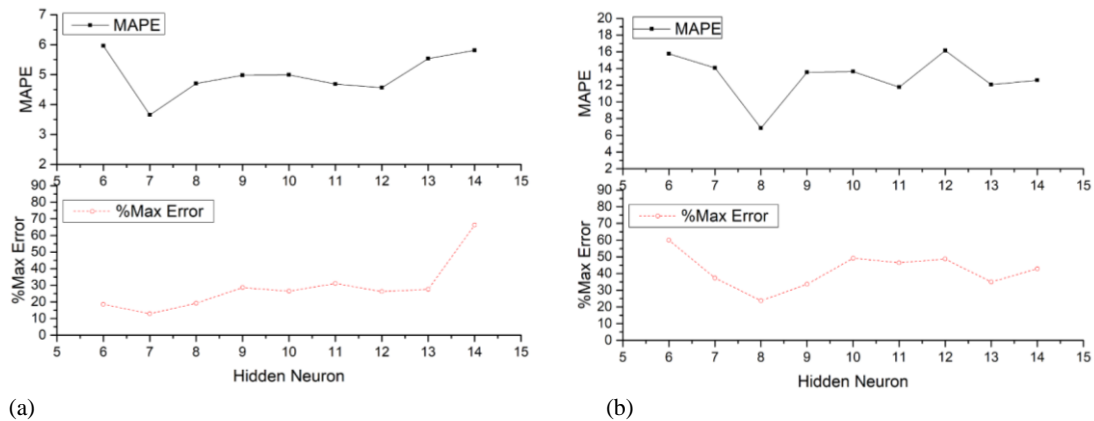(a)   (b)

Fig. 5. Best MAPE values depending on numbers of hidden neuron for (a)lift coefficient and (b)drag coefficient.

nh/2, respectively. As it can be seen from Fig. 5a, the MSE and MAPE (defined by Eqs. (3) and (4)) are determined for the best fit training results by using MATLAB (MATLAB version 9a, 2009). The best fit for the lift coefficient training is achieved at MAPE = 3.657, MSE=0.00107 and for testing MSE=0.00057, MAPE=2.718. The maximum estimation error is observed (12.84) at settings Re=50000, x_c/C=0.4, AoA=2 as can be seen in Fig. 8.

As can be seen from Fig. 5b, the MSE and MAPE (defined by Eqs. (3) and (4)) are determined for the best fit training results by using MATLAB (2009). The best fit for the drag coefficient training is achieved at MAPE = 6.855, MSE=0.0027 and for testing MSE=0.0026, MAPE=7.187. The maximum estimation error is observed (23.705) at settings Re=40000, x_c/C=0.1, AoA=7 as can be seen in Fig. 14.
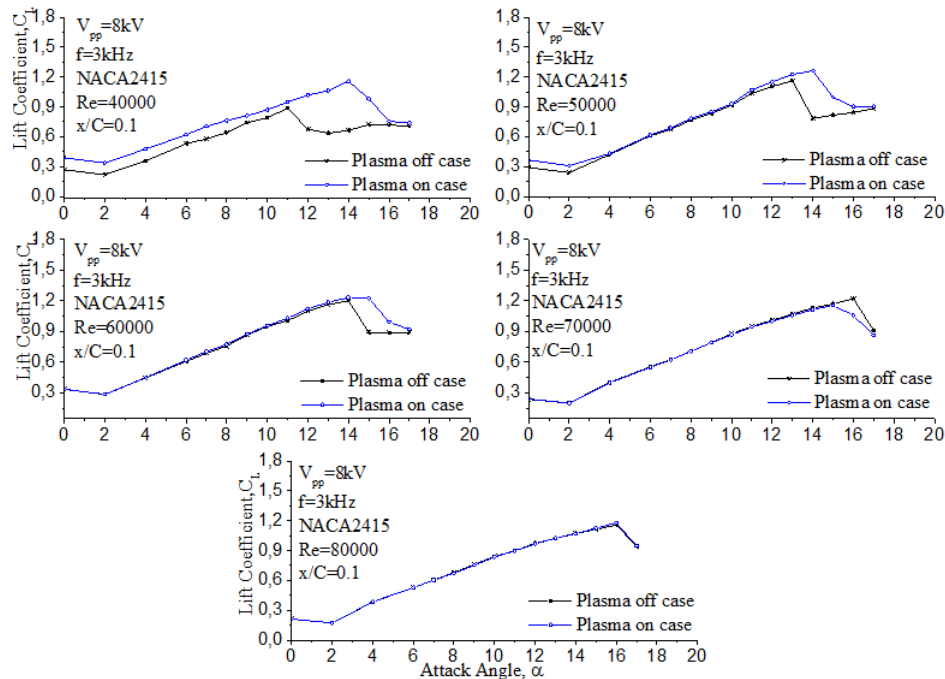
1170

H. Akbıyık and H. Yavuz / *JAFM*, Vol. 14, No. 4, pp. 1165-1181, 2021.

Fig. 6. Comparison of plasma on case and base NACA 2415 airfoil lift coefficient results for various Reynolds number at $x_c/C=0.1$.

3. RESULTS AND DISCUSSIONS

The previously presented ANN model is used to predict the lift and drag coefficient for the selected cases. In order to be able to provide a full picture for the aerodynamic coefficients (lift and drag) under different working conditions, the experiments are performed for a range of Reynolds number (from 40 000 to 80000), plasma actuator positions (from $x_c/C=0.1$ to 0.5), and angle of attack (from 0 to 17). Hence, in total 1150 experiments are performed and related aerodynamic coefficients (lift and drag) are determined. With the use of the data and the trained ANN, it is now possible to determine the aerodynamic coefficients for any given working condition provided that they are within the mentioned range.

In Fig. 6, the lift force coefficients acting on a NACA 2415 airfoil is experimented for various Reynolds number and plasma actuator positions. It is clearly seen that plasma actuators are effective devices for flow control around an airfoil. The comparison of the lift coefficients of "plasma on case" and "base airfoil case" shows that the plasma actuators increases the lift coefficient for in the range of Reynolds number between 40000 and 70000. For the Reynolds number of 80000, it is worth mentioning that plasma actuators are not effective to reattach the separated flow. This is due to the low velocity profile of induced flow.

When AoA increased at the Reynolds number being varied between 40 000 and 70 000, the flow fails to follow the surface of the airfoil for the critical angle. In this Reynolds number range, for the cambered airfoils (6% or above), the flow regime is

observed to be a laminar separation with transition to turbulent flow form. In this Reynolds number range between 70 000 and 200 000, the flow regime is observed to be extensive laminar form. At this point the airfoil performance is affected by the Laminar Separation Bubble. Hence, the Laminar Separation Bubble contributes to separation of the flow from the airfoil surface depending on properties of the bubble. At the case of Reynolds number of 80 000, the induced flow fails to reattach the separated flow. Thus, the stall angle is not shifted further and no aerodynamic performance improvement is achieved. Apart from the case for Reynolds number of 80 000, as it can be seen from Fig. 6, the stall angle has been shifted with the plasma actuator contribution to aerodynamic performance.

Figure 7 shows that the ANN model generated estimation values are considerably matched up with the experimental data indicating highly satisfactory results. With reference to the base airfoil, the improvement in the lift coefficient is observed at certain positions of the plasma actuators. Also, in the figure it can be seen that the stall angle has been shifted for all x_c/C positions except for $x_c/C=0.2$. Predicted values of the lift coefficient overlap with experimental ones even at the stall angle values. As can be seen from Fig. 8, for $x_c/C=0.1$, the lift coefficient at $\alpha = 14°$ is 1.273 while estimated value is 1.263. For $x_c/C=0.2$, the lift coefficient at $\alpha = 13°$ is 1.112 while estimated value is 1.118. For $x_c/C=0.3$, the lift coefficient at $\alpha = 14°$ is 1.171 while estimated value is 1.168. For $x_c/C=0.4$, the lift coefficient at $\alpha = 14°$ is 1.112 while estimated value is 1.132. For $x_c/C=0.5$, the lift coefficient at $\alpha = 14°$ is 1.06 while estimated value is 1.051.
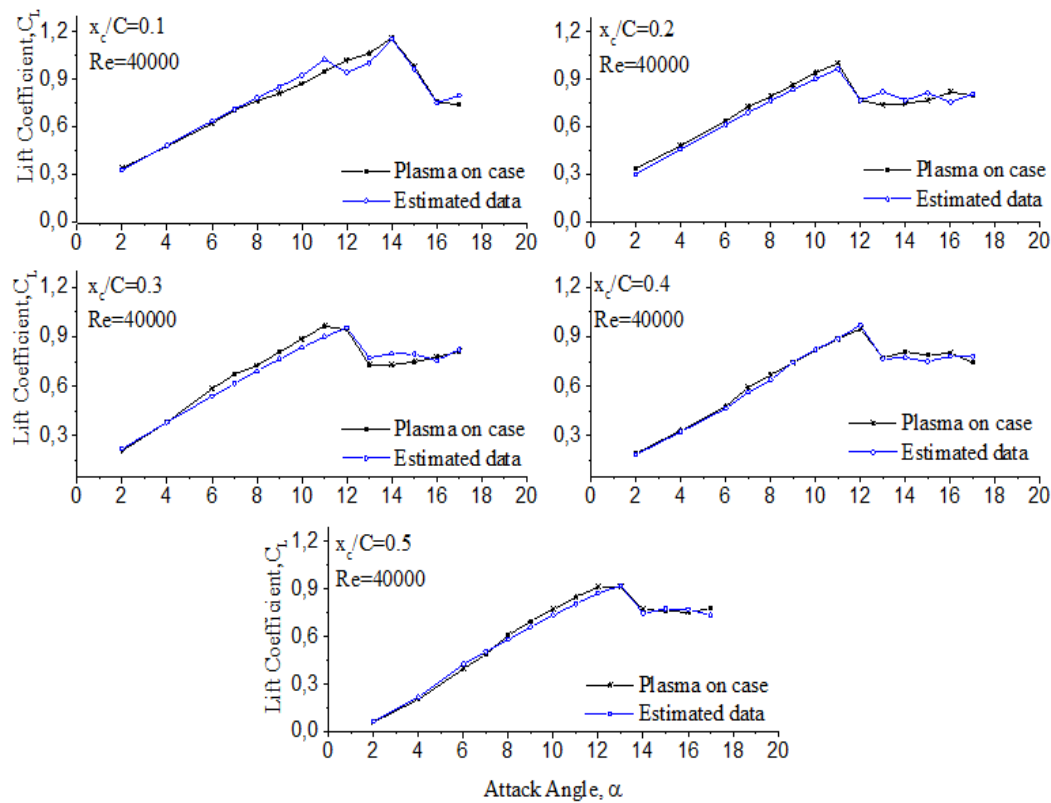
Fig. 7. Comparison of experimental and estimated lift coefficients of a NACA 2415 airfoil for various plasma actuator positions (x_c/C) at Reynolds number of 40000.

These results prove the validity of the proposed ANN model estimations used in determination of lift coefficient of the airfoil. Hence, the proposed ANN based aerodynamic lift coefficient estimation technique is very much useful in determination of performance with highly accurate results. This also allows the user to achieve any aerodynamic lift coefficient estimation for any given working condition without performing any experiment.

As shown in Fig. 9, for the Reynolds number of 60 000, it is seen that plasma actuators have been effective in shifting the stall angle. It is observed that it does not contribute to the lift coefficient for the pre-stall attack angle while it has been effective in improving the lift coefficient for post-stall cases. In Fig. 9, considering the lift coefficient curve for the estimated values, the maximum error is observed at $x_c/C=0.3$ plasma actuator position. All in all, it can be said that the proposed ANN based estimation model produces results that matches the experimental data based aerodynamic performance curves successfully in the pre-stall, stall and post-stall states.

As can be seen in Fig. 6 to 10, the variation of the Reynolds number plays an important role in effectiveness of the plasma actuators on the aerodynamic performance of the airfoil. In general,

the proposed ANN aerodynamic estimation model is very much successful for prediction of the lift coefficient up to the stall angle where the lift coefficient is almost linear. On the other hand, although the model estimates the lift coefficient within a certain range of error it performs relatively poorly. For the base airfoil study presented in Fig. 6, the stall angle is shifted about 1 degree for the actuator position of $x_c/C=0.1$. It is seen that the separated flow with the variation of actuator position is more effective in shifting the stall angle in the positions of $x_c/C = 0.3$ and 0.5, where the separated flow becomes closer to the surface. In the actuator position of $x_c/C = 0.4$, the actuator's effectiveness decreases as it remains inside the flow separation area.

As seen in Fig. 11, when the Reynolds number exceeds 80000, the efficiency of plasma actuators decreases as the position approaches $x_c/C=0.5$. In this case, the stall angle shift is about 5°. However, no improvement in the lift coefficient is observed. Fig. 12 presents the full data set used in predicting the lift coefficient where training and testing subsets are also presented. The results indicate that the estimation matches the experimental data. The percentage error, defined as difference between measured and predicted values, is observed to be about 12.84 for the maximum error case.
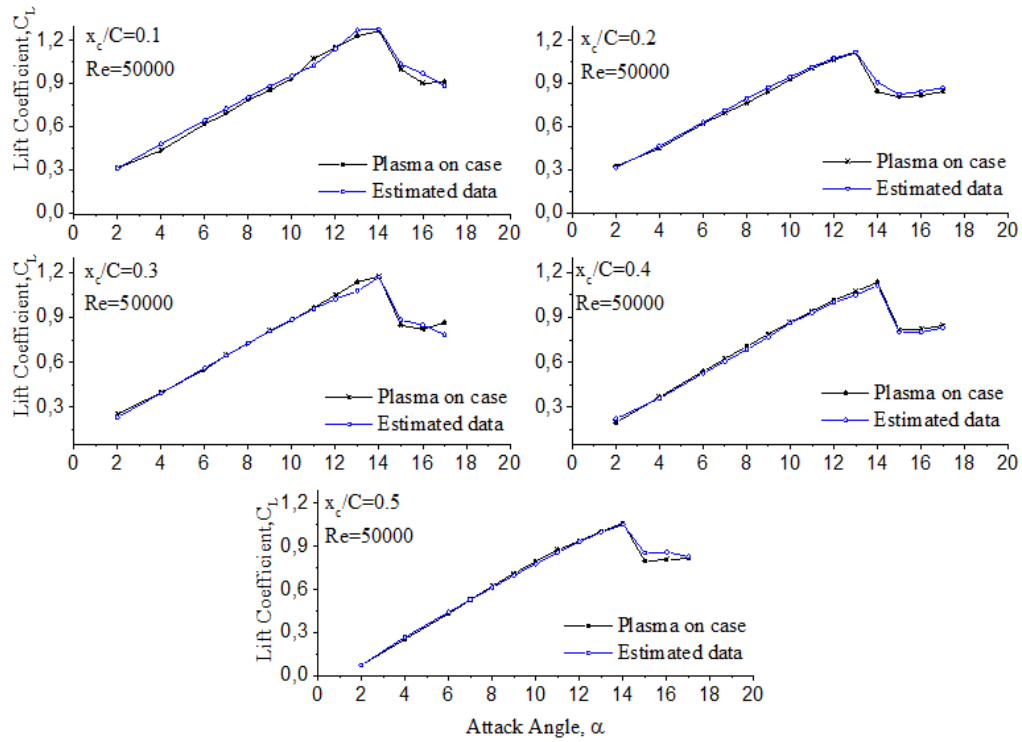
H. Akbıyık and H. Yavuz / *JAFM*, Vol. 14, No. 4, pp. 1165-1181, 2021.

Fig. 8. Comparison of experimental and estimated lift coefficients of a NACA 2415 airfoil for various plasma actuator positions (x_c/C) at Reynolds number of 50000.
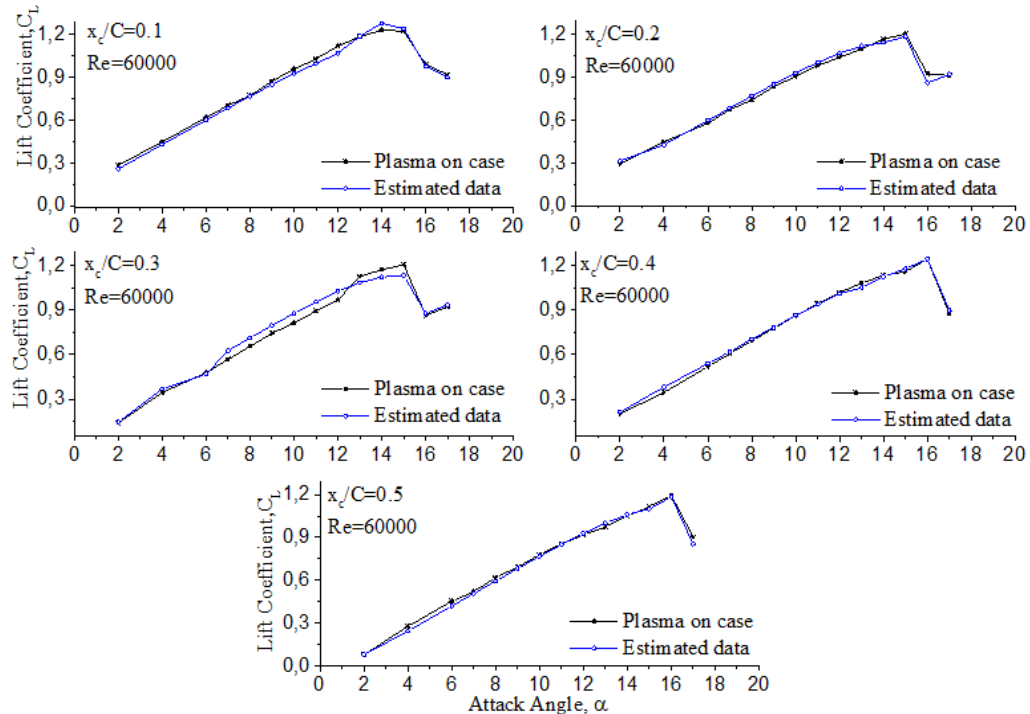
Fig. 9. Comparison of experimental and estimated lift coefficients of a NACA 2415 airfoil for various plasma actuator positions (x_c/C) at Reynolds number of 60000.
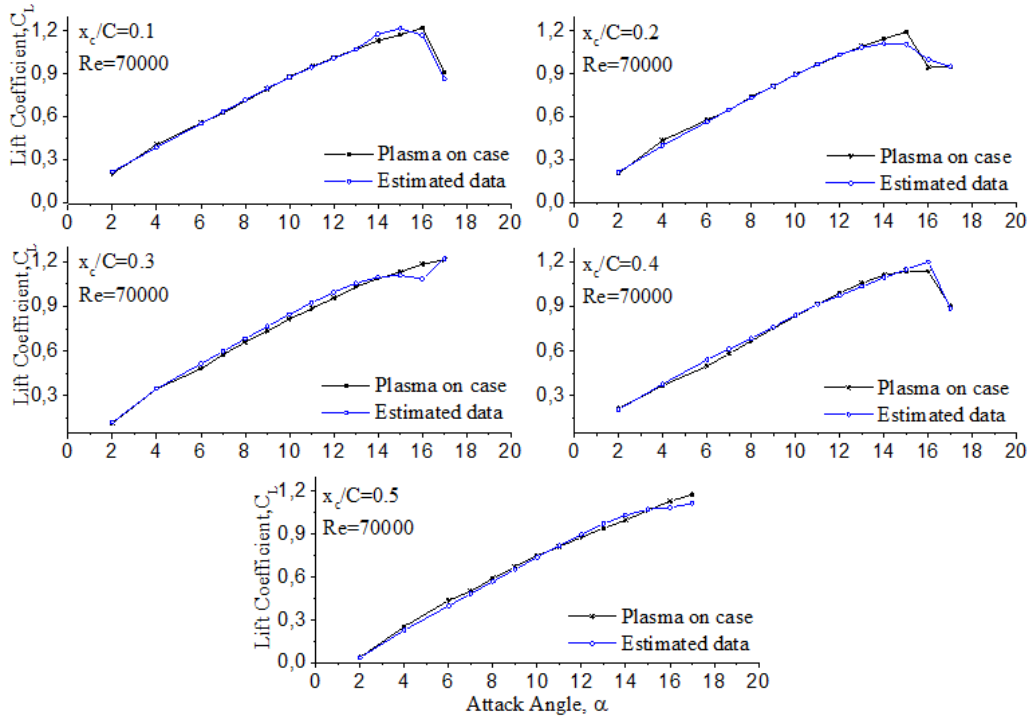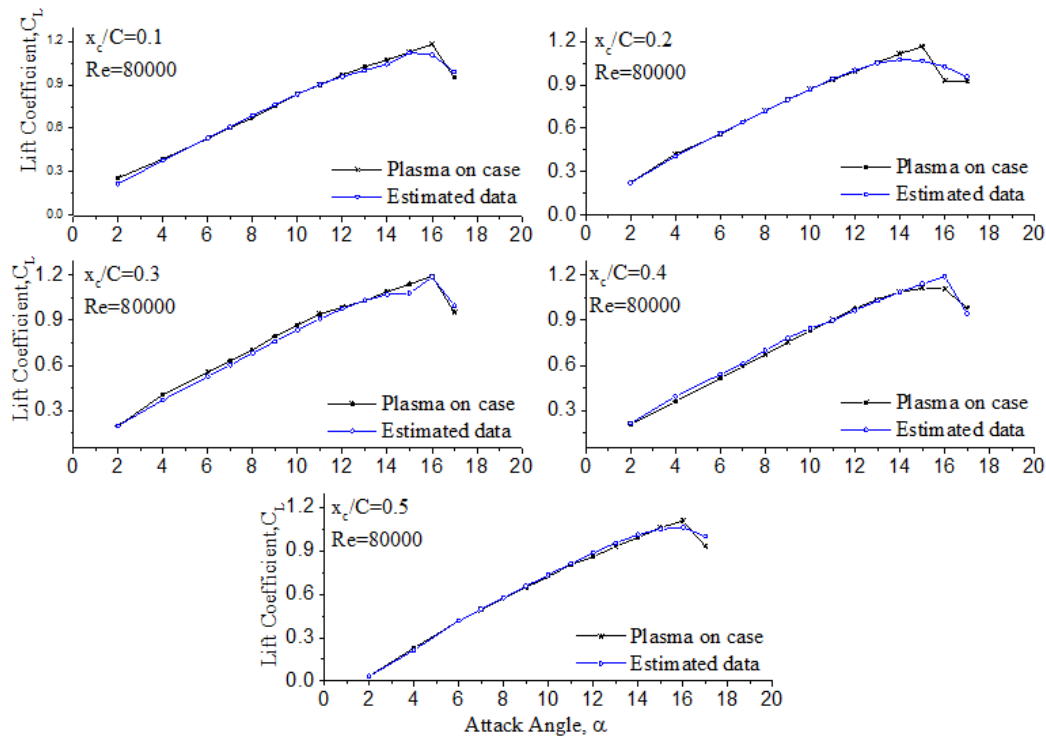
1173

Fig. 10. Comparison of experimental and estimated lift coefficients of a NACA 2415 airfoil for various plasma actuator positions (x_c/C) at Reynolds number of 70000.

Fig. 11. Comparison of experimental and estimated lift coefficients of a NACA 2415 airfoil for various plasma actuator positions (x_c/C) at Reynolds number of 80000.
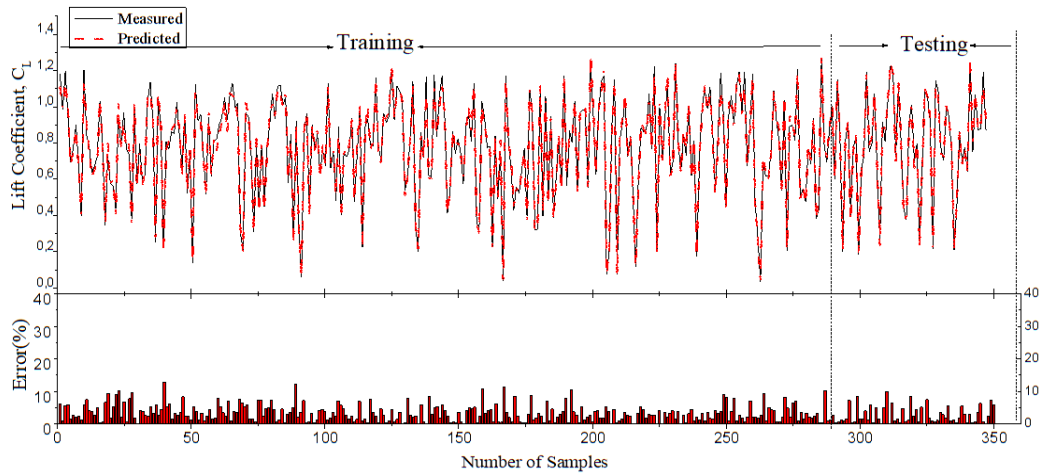
1174

Fig. 12. Percentage error between measured and predicted lift coefficient values in proposed ANN model.

All in all, it can be said that the proposed ANN based estimation model produces results that matches the experimental data based aerodynamic performance curves successfully in the pre-stall, stall and post-stall states. In this study, it is shown that the proposed ANN aerodynamic performance estimation model is seen to be a sufficient and successful tool for modeling the flow control effects of the plasma actuators. Considering the nonlinear relationships amongst the input parameters (plasma actuator position, Reynolds number, AoA) and output parameters (lift and drag coefficient) highly encouraging and satisfactory results are obtained by the proposed ANN model. Besides, for a better ANN aerodynamic performance estimation model, aerodynamic flow conditions, airfoil geometry and plasma actuator electrical performance parameters could be added as input parameters. In addition, the

number of hidden layers, the input function (other than tansig) etc. could be used to improve performance of ANN aerodynamic performance estimation model. The drag coefficients of the base airfoil and the airfoil model with plasma actuator are compared for different Reynolds number and various plasma actuator positions as shown in Fig. 13. For low Reynolds number the curves of the drag coefficient are nearly linear before the stall angle. Then, these curves are increased dramatically. It appears that the plasma actuators reduce drag coefficient of the base airfoil effectively, at Reynolds numbers of 40000 and 50000. However, it is observed that the plasma actuators reduce the drag coefficient beyond the AoA of 14° at Re=60000 and 70000. On the other hand, there does not seem to have a significant reduction in drag for Re number of 80000.
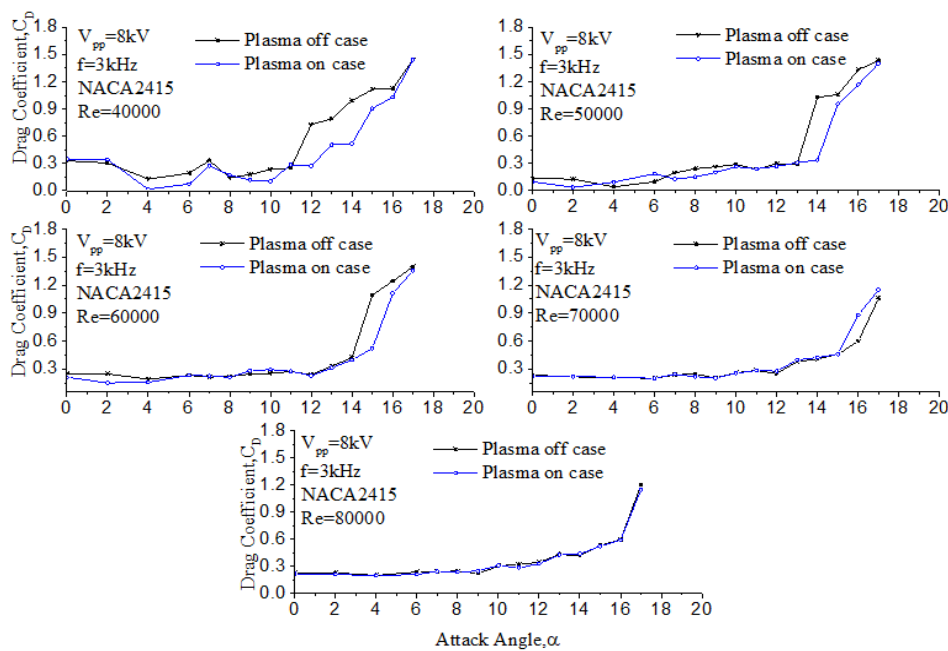

Fig. 13. Comparison of plasma on case and base NACA 2415 airfoil drag coefficient results for various Reynolds number at x_c/C=0.1.

Figure 14 shows the comparison of ANN estimated drag coefficient and the base airfoil drag coefficient for various plasma actuator positions. With the use of plasma actuators at the positions of $x_c/C = 0.2$ and 0.3, an improvement in the lift coefficient is observed at low angle of attack values. However, in the case of the plasma actuators positions of $x_c/C = 0.4$ and 0.5, the situation in drag coefficient is increased. The results presented in the figure for the drag coefficient indicates that the ANN based estimated the drag coefficient results sufficiently match the experimental values.

In Fig. 15, it is seen that plasma actuators do not contribute to drag reduction when placed at positions from leading edge to mid chord. The maximum reduction in drag is observed when plasma actuators are placed near the leading edge of the airfoil. It is reported in the study by Karasu *et al.* (2012) that the laminar separation bubble may occur after angle of attack of 4°. Besides, the laminar separation bubble length in this case is about 0.4 x_c/C at Re=50000 for NACA2415 airfoil. They also concluded that the laminar separation bubble lengths are 0.3 x_c/C and 0.18 x_c/C for the attack angle of 10° and 12°, respectively. Therefore, the effectiveness of the plasma actuators is not enough to reattach the separated flow from the surface of the airfoil. There is no significant improvement for drag reduction at Re 50000 for $x_c/C=0.1$ when angle of attack is between 10° and 13°. Nevertheless, the aerodynamic performance is improved with regards to C_L/C_D when this case is assessed for lift coefficient. The results presented in Fig. 15 illustrates the experimental and estimated values of drag coefficient. It can be said that the proposed ANN based estimation model generates very much successfully matched results.

In Fig. 16, for various plasma actuator positions ($x_c/C = 0.1, 0.2, ., 0.5$), the drag coefficient related results are presented for a range of AoA. It can be seen in Fig. 6 that the stall occurs at Reynolds number of 60 000 and $\alpha=14°$. In Fig. 16, before this attack angle, drag coefficient curve nearly linear. However, after stall angle, curve is increased dramatically. The application of plasma actuators is not effective in reduction of drag coefficient for Re=60 000 and further. The experimental results presented in Fig. 16 illustrates a linear and a nonlinear region for each plot. The linear results are up to the stall angle of 14°. However, the nonlinear region is the one after the stall angle. The presented results show that the proposed ANN model matches the experimental results very well indicating that ANN is well trained. Figure 17 presents the full data set used in predicting the drag coefficient where subsets of training and testing sections of the full dataset is presented. The results related to percentage error, for pre-stall, near-stall and post-stall case, are presented as the difference between measured and predicted values for the drag coefficient of a NACA 2415 airfoil. The maximum error for the pre-stall case is observed about 23.705% at $x_c/C=0.1$, the Reynolds number of 40 000 and $\alpha=7°$. The maximum error for the near-stall case is observed about 16.85% at $x_c/C=0.2$, the Reynolds number of 40 000 and $\alpha=12°$. The maximum error for the post-stall case is observed about 16.887% at $x_c/C=0.3$, the Reynolds number of 60 000 and $\alpha=16°$. The presented results of the study indicate that the developed ANN model can be used to determine aerodynamic performance coefficients under different conditions without the need of experimental study that requires highly time consuming and costly experimental studies.
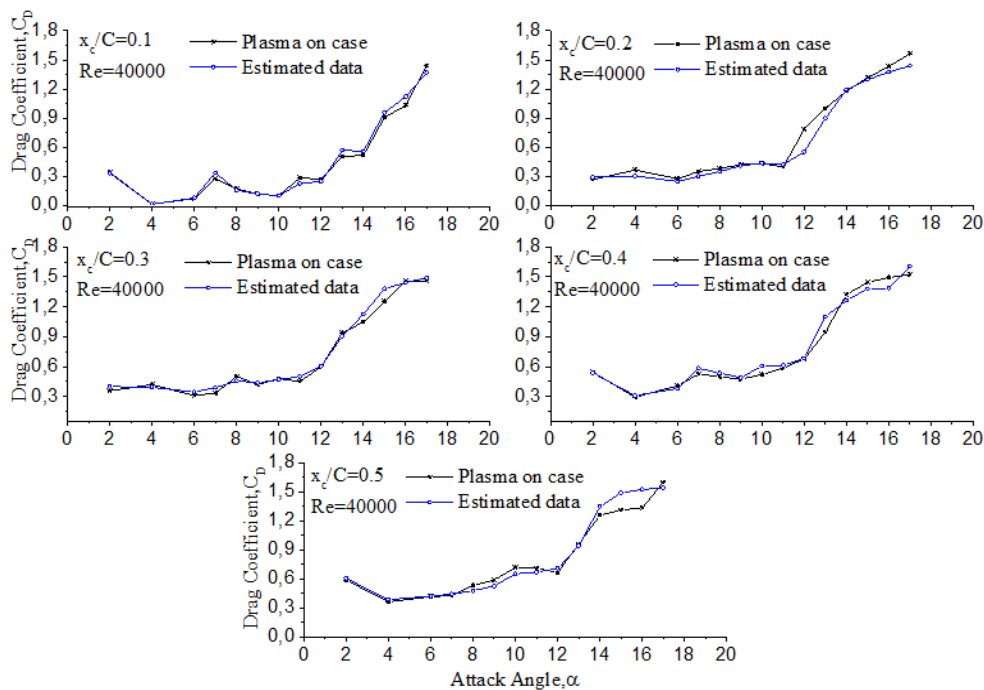

Fig. 14. Comparison of experimental and estimated drag coefficients of a NACA 2415 airfoil for various plasma actuator positions (x_c/C) at Reynolds number of 40000.
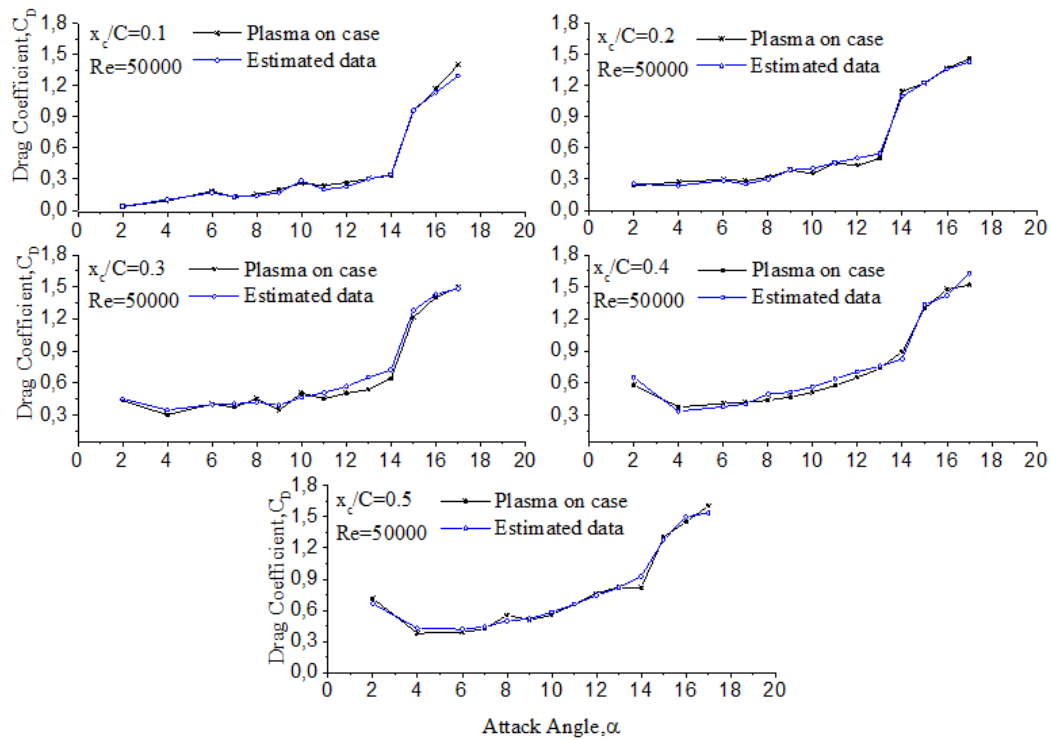
Fig. 15. Comparison of experimental and estimated drag coefficients of a NACA 2415 airfoil for various plasma actuator positions (x_c/C) at Reynolds number of 50000.
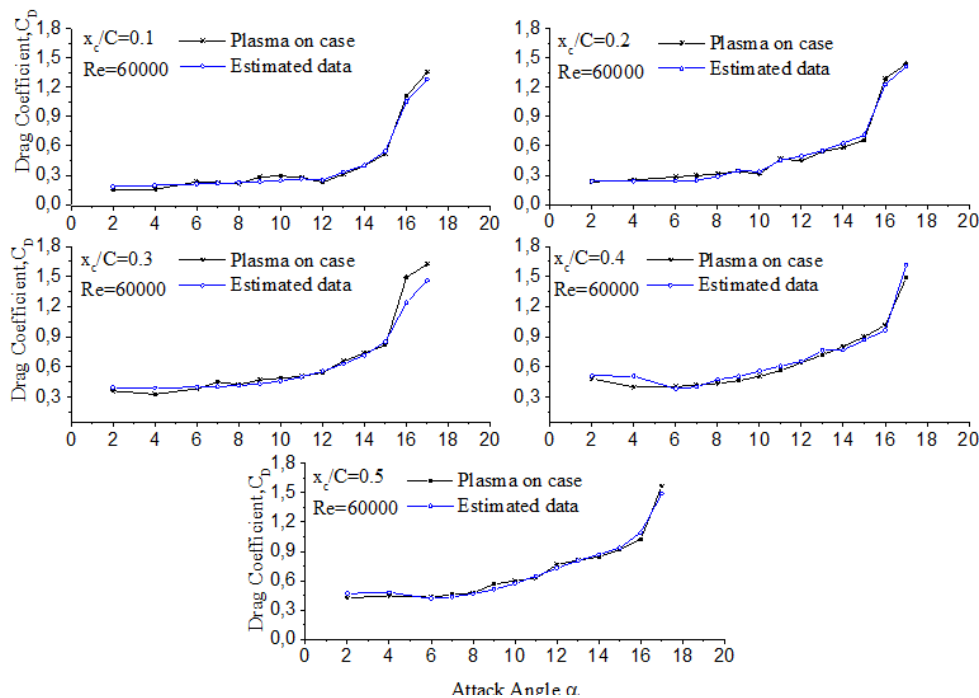

Fig. 16. Comparison of experimental and estimated drag coefficients of a NACA 2415 airfoil for various plasma actuator positions (x_c/C) at Reynolds number of 60000.

5. CONCLUSION

In this study, an ANN model used as a successful tool for modelling of plasma actuators as an active device in flow control method. The trained model is then used to predict the aerodynamic force coefficients (lift and drag) of a NACA 2415 airfoil for various AoA, Reynolds numbers and plasma actuator positions between leading edge and mid-chord. This ANN based estimation model provides numerous advantages such as qick achievement of results at almost no cost. Besides, the ANN based
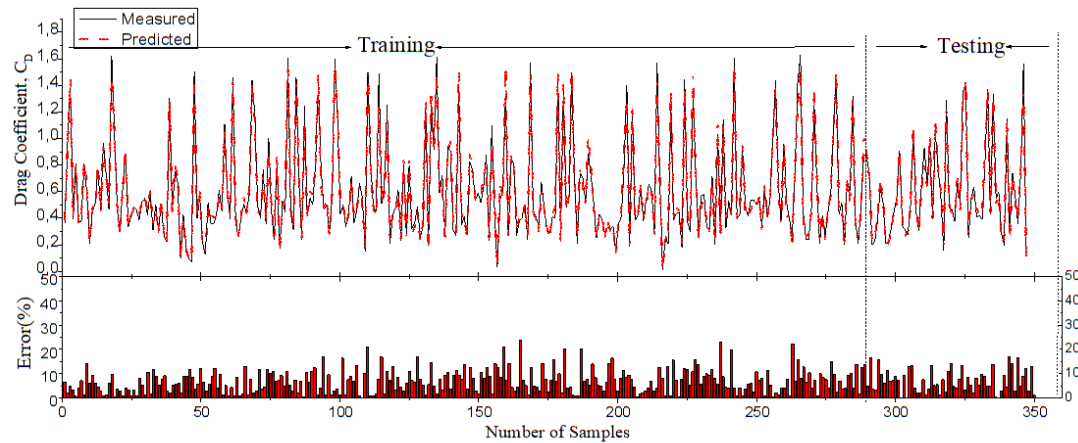
1177

Fig. 17. Percentage error between measured and predicted drag coefficient values in proposed ANN model.

approach does not require any experimental study provided that the aerodynamic coefficient related working conditions are within the range of input parameters of this study. Another important contribution of the proposed ANN model is to provide extensive results covering a wide range of input settings providing details on use of the plasma actuators for active flow control in aerodynamics. In other words, the overall results presented maps the effects of plasma actuators in active flow control around a NACA 2415. It is observed that the plasma actuators increase the lift coefficient of the airfoil for Reynolds number between 40 000 and 60 000. However, there is no significant improvement in lift coefficient for Reynolds number of 70 000 and 80 000. The stall angle is shifted for all Reynolds number except for Reynolds number of 80 000. The drag coefficient of the airfoil is decreased for Reynolds number between 40 000 and 60 000. From a wider perspective, the decrease in drag coefficient and increase in lift coefficient leads to enhancement of C_L/C_D ratio compared with the base airfoil case. It is also worth mentioning that varying the plasma actuators positions affects the efficiency of plasma actuators in flow control around the airfoil. The presented results indicate that the predicted and experimental values are compared and the results well matched. So, it is suggested that the results of the present study can be used in the applications of plasma actuators in active flow control for aerodynamics of a NACA 2415 airfoil in general. For further studies, varying the effectiveness of plasma actuators (such as electrical parameters of the plasma) may be considered for a better ANN model. In addition, the structures of the actuators (such as dielectric material type, gap between the electrodes and so on) could also be studied for future works.

ACKNOWLEDGEMENTS

REFERENCES

Akbıyık, H., H. Yavuz and Y. E. Akansu (2017). Comparison of the linear and spanwise-segmented DBD plasma actuators on flow control around a NACA0015 airfoil. *IEEE Transactions on Plasma Science* 45, 2913-2921.

Beck, A., D. Flad and D. Munz (2019). Deep neural networks for data-driven LES closure models. *Journal of Computational Physics* 398, 1-23.

Belus, V., J. Rabault, J. Viquerat, Z. Che, E. Hachem and U. Reglade (2019). Exploiting locality and translational invariance to design effective deep reinforcement learning control of the 1-dimensional unstable falling liquid film. *AIP Advances* 9, 125014.

Bishop, C. M. (1994). Neural networks and their applications, *Review of Scientific Instruments* 65, 1803-1832.

Calise, A. J. and R. T. Rysdyk (1998). Nonlinear adaptive flight control using neural networks. *IEEE Control Systems Magazine* 18, 14-25.

Cai, S., J. Liang, S. Zhou, Q. Gao, C. Xu, R. Wei, S. Wereley and J. S. Kwon (2019). Deep-PIV: a new framework of PIV using deep learning techniques. *13th International Symposium on Particle Image Velocimetry*. Munich, Germany.

Cattafesta, L. N. III, D. Shukla, S. Garg and J. A. Ross (1999). Development of an adaptive weapons-bay suppression system. *AIAA Aeroacoustics Conference. Paper No*: 99-1901.

Chow, R. and C. P. Van Dam (2011). Inboard stall and separation mitigation techniques on wind turbine rotors. *49th AIAA Aerospace Sciences*

Meeting including the New Horizons Forum and Aerospace Exposition. Paper No: 2011-152.

Corke, T. C., E. J. Jumper, M. L. Post, D. Orlov and T. E. McLaughlin (2002). Application of weakly-ionized plasmas as wing flow-control devices. *40th AIAA Aerospace Sciences Meeting & Exhibit. Paper No*: 2002-0350.

Dalvand, S. E., M. Ebrahimi and S. G. Pouryoussefi (2018). Experimental investigation, modelling and prediction of transition from uniform discharge to filamentary discharge in DBD plasma actuators using artificial neural network. *Applied Thermal Engineering* 129, 50-61.

Dickenson, M. H., F. O. Lehmann and S. P. Sane (1999). Wing rotation and the aerodynamic basis of insect flight. *Science* 284, 1954-1960.

Dorn, M. (1989). Aircraft agility: The science and the opportunities. *AIAA/AHS/ASEE Aircraft Design. Systems and Operations Conference. Paper No*: 89-2015.

Durhasan, T., E. Pınar, G. M. Özkan, M. M. Aksoy, H. Akıllı and B. Şahin (2018). PIV measurement downstream of perforated cylinder in deep water. *European Journal of Mechanics B-Fluid* 72, 225-234.

Faller, W. E., S. J. Shcreck, and M. W. Luttges (1994). Real-time prediction and control of three dimensional unsteady separated flow fields using neural networks. *32nd Aerospace Sciences Meeting & Exhibit. Paper No:* 94-0532.

Fernández-Gámiz, U. (2013). Fluid dynamic characterization of vortex generators and two-dimensional turbulent wakes. Ph. D. thesis, the Polytechnic University of Catalonia, Barcelona, Spain.

Fouatih, O. M., M. Medale, O. Imine, and B. Imine (2016). Design optimization of the aerodynamic passive flow control on NACA 4415 airfoil using vortex generators. *European Journal of Mechanics B Fluids* 56, 82-96.

Gad-El-Hak, M. (2000). *Flow control: passive, active and reactive management*. Cambridge: Cambridge University Press.

Gim, Y., D. K. Jang, D. K. Sohn, H. Kim and H. S. Ko (2020). Three-dimensional particle tracking velocimetry using shallow neural network for real-time analysis. *Experiments in Fluids* 61(26), 1-8.

Güler, A. A., M. Seyhan and Y. E. Akansu (2018). Effect of signal modulation of DBD plasma actuator on flow control around NACA0015. *Journal of Thermal Science and Technology* 38, 95-105.

Gunther, B., F. Thiele, R. Petz, W. Nitsche, J. Sahner, T. Weinkauf and H. C. Hege (2007). Control of separation on the flap of a three-element high-lift configuration. *45th AIAA*

Aerospace Sciences Meeting and Exhibit. Paper No: 2007-265.

Hagan, M. T. and M. B. Menhaj (1994). Training feed-forward neural networks with the Marquardt algorithm. *IEEE Transactions on Neural Networks* 5, 989-993.

Hand, B., G. Kelly and A. Cashman (2017). Numerical simulation of a vertical axis wind turbine airfoil experiencing dynamic stall at high Reynolds numbers. *Computers & Fluids* 149, 12-30.

Hecht-Nielsen, R. (1990). *Neurocomputing*. Addison-Wesley, Menlo Park, CA.

Hezaveh, S. H., E. Bou-Zeid, M. W. Lohry and L. Martinelli (2017). Simulation and wake analysis of a single vertical axis wind turbine. *Wind Energy* 20, 713-730.

Hornik, K., M. Stinchcombe and H.. White (1989). Multilayer feedforward networks are universal approximators. *Neural Networks* 2(5), 359-366.

Huang, X. and X. Zhang (2010). Plasma actuators for noise control. *International Journal of Aeroacoustics* 9, 674-704.

Hunt, K. J., D. Sbarbaro, R. Zbikowski and P. J. Gawthrop (1992). Neural networks for control systems-A survey. *Automatica* 28, 1083-1112.

Jolibois, J., M. Forte and E. Moreau (2008). Application of an AC barrier discharge actuator to control airflow separation above a NACA 0015 airfoil: Optimization of the actuation location along the chord. *Journal of Electrostatics* 66, 496-503.

Kang, S. (1991). *An investigation of the use of feedforward neural networks for forecasting*. Ph.D. Thesis, Kent State University. US.

Karasu, İ., M. S. Genç, H. H. Açıkel and M. T. Akpolat (2012). An experimental study on laminar separation bubble and transition over an aerofoil at low Reynolds number. *30th AIAA Applied Aerodynamics Conference. Paper No*: 2012-3030.

Kurtulus, D. F. (2009). Ability to forecast unsteady aerodynamic forces of flapping airfoils by artificial neural network. *Neural Computing & Applications* 18, 359-368.

Linse, D. J. and R. F. Stengel (1993). Identification of aerodynamic coefficients using computational neural networks. *Journal of Guidance, Control, and Dynamics* 16, 1018-1025.

Lippmann, R. P. (1987). An introduction to computing with neural nets. *IEEE ASSP Magazine* 4, 4-22.

Lissaman, P. B. S. (1983). Low-Reynolds-number airfoils. *Annual Review of Fluid Mechanics* 15, 223-239.

MATLAB version 9a. (2009). The MathWorks Inc 3

Apple Hill Drive Massachusetts.

Mazaheri, K., J. Omidi and K. C. Kiani (2016). Simulation of DBD plasma actuators effect on aerodynamic performance improvement using a modified phenomenological model. *Computers & Fluids* 140, 371-384.

Meng, X., H. Hu, X. Yan, F. Liu and S. Luo (2018). Lift improvements using duty-cycled plasma actuation at low Reynolds numbers. *Aerospace Science and Technology* 72, 123-133.

Messanelli, F., E. Frigerio, E. Tescaroli and M. Belan (2019). Flow separation control by pulsed corona actuators. *Experimental Thermal and Fluid Science* 105, 123-135.

Moreau, E. (2007). Airflow control by non-thermal plasma actuators. *Journal of Physics D: Applied Physics* 40, 605-636.

Moreau, E., C. Louste, G. Artana, M. Forte and G. Touchard (2006). Contribution of plasma control technology for aerodynamic application. *Plasma Processes & Polymers* 3, 697-707.

Mueller, T. J. (1999). *Aerodynamic measurements at low Reynolds numbers for fixed wing micro-air vehicles. Development and Operation of UAVs for Military and Civil Applications*. Hessert Center for Aerospace Research University of Notre Dame.

Narendra, K. S. (1990). Identification and control of dynamical systems using neural networks. *IEEE Transactions on Neural Networks* 1, 4-27.

Özşahin, S. and M. Murat (2018). Prediction of equilibrium moisture content and specific gravity of heat treated wood by artificial neural networks. *European Journal of Wood and Wood Products* 76, 563-572.

Post, M. L. and T. C. Corke (2004). Separation control on high angle of attack airfoil using plasma actuators. *AIAA J ournal* 42, 2177-2184.

Post, M. L. and T. C. Corke (2006). Separation control using plasma actuators: Dynamic stall vortex control on oscillating airfoil. *AIAA Journal* 44, 3125-3135.

Rabault, J., J. Kolaas and A. Jensen (2017). Performing particle image velocimetry using artificial neural networks: a proof-of-concept. *Measurement Science and Technology* 28, 1-14.

Rabault, J., M. Kuchta, A. Jensen, U. Réglade and N. Cerardi (2019). Artificial neural networks trained through deep reinforcement learning discover control strategies for active flow control. *Journal of Fluid Mechanics* 865, 281-302.

Rabault J. and A. Kunhle (2019). Accelerating deep reinforcement learning strategies of flow control through a multi-environment approach. *Physics of Fluids* 31(9), 094105.

Rai, M. M. and N. K. Madavan (2001). Application of artificial neural networks to the design of turbomachinery airfoils. *Journal of Propulsion and Power* 17, 176-183.

Rokhsaz, K. and J. E. Steck (1993b). Application of artificial neural networks in nonlinear aerodynamics and aircraft design. *SAE Technical Paper Series.*

Rokhsaz, K. and E. J. Steck (1993a) Use of neural networks in control of high-alpha maneuvers. *Journal of Guidance, Control, and Dynamics* 16, 934-939.

Roth, J. R., D. M. Sherman and S. P. Wilkinson (1998). Boundary layer flow control with a one atmosphere uniform glow discharge surface plasma. *Aerospace Sciences Meeting & Exhibit. Paper* No: 98-0328.

Roth, J. R., D. M. Sherman and S. P. Wilkinson, (2000). Electrohydrodynamic flow control with a glow-discharge surface plasma. *AIAA Journal* 38, 1166-1172.

San, O. and R. Maulik (2018). Neural network closures for nonlinear model order reduction. *Advances in Computational Mathematics* 44, 1717-1750.

Sarıoğlu, M., M. Seyhan and Y. E. Akansu (2016). Drag force estimation of a truck trailer model using artificial neural network. *International Journal of Automotive Engineering and Technologies* 4, 168-175.

Schreck, S. J., W. E. Faller and M. W Luttges (1995). Neural network prediction of three-dimensional unsteady separated flow field. *Journal of Aircraft* 32, 178-185.

Seyhan, M., Y. E. Akansu, M. Murat, Y. Korkmaz, S. O. Akansu (2017). Performance prediction of PEM fuel cell with wavy serpentine flow channel by using artificial neural network. *International Journal of Hydrogen Energy* 42, 25619-25629.

Skapura, D. M. (1996). *Building neural networks*, Addison-Wesley Professional, Menlo Park.

Smith, B. L. and A. Glezer (1997). Vectoring and small-scale motions effected in free shear flows using synthetic jet actuators. *35th AIAA Aerospace Sciences Meeting. AIAA paper no*: 97-0213.

Stiesdal, H. and P. B. Enevoldsen (2003). Flexible serrated trailing edge for wind turbine rotor blade. Siemens. European Patent Office, EP 1 314 885 B1.

Tang, H., J. Rabault, A. Kuhnle, Y. Wang and T. Wang (2020). Robust active flow control over a range of Reynolds numbers using an artificial neural network trained through deep reinforcement learning. *Physics of Fluids* 32, 053605.

Tang, Z. and P. A. Fishwick (1993). Feedforward neural nets as models for time series

H. Akbıyık and H. Yavuz / *JAFM*, Vol. 14, No. 4, pp. 1165-1181, 2021.

forecasting. *ORSA Journal on Computing* 5, 374-385.

Wang, J. J., K. S. Choi, L. H. Feng, T. N. Jukes and R. D. Whalley (2013). Recent developments in DBD plasma flow control. *Progress in Aerospace Sciences* 62, 52-78.

Winslow, J., H. Otsuka, B. Govindarajan and I. Chopra (2018). Basic understanding of airfoil characteristics at low Reynolds number (10^4-10^5). *Journal of Aircraft* 55, 1050-1061.

Winzen, A., B. Roidl, S. Klän, M. Klaas and W. Schröder (2014). Particle-Image velocimetry and force measurements of leading edge-serrations on owl-based wing models. *Journal of Bionic Engineering* 11, 423-438.

Wong, F. S. (1991). Time series forecasting using backpropagation neural networks. *Neurocomputing* 2, 147-159.

Yen, D. T., C. P. Van Dam, F. Bräuchle, R. L. Smith and S. D. Collins (2000). Active Load Control and Lift Enhancement Using MEM Translational Tabs. *Proceedings of the Fluids Conference and Exhibit AIAA*, pp. 2000-2422.

Zhu, H., W. Hao, C. Li, Q. Ding and B. Wu (2019). Application of flow control strategy of blowing, synthetic and plasma jet actuators in vertical axis wind turbines. *Aerospace Science and Technology* 88, 468-480.